Strong Motion Simulation in Tehran Using Empirical Green Function Method

Ebrahim Haghshenas[1] and Pierre-Yves Bard[2]

1. Geotechnical Engineering Research Center, International Institute of Earthquake Engineering and Seismology (IIEES), Tehran, I.R. Iran, e-mail: haghshen@iiees.ac.ir
2. LGIT Observaotire de Grenoble, France

ABSTRACT: *The Empirical Green Function (EGF) technique, using the small earthquakes, recorded by a temporary seismological network, was applied to estimate the effect of the strong seismic motions, due to probable future great earthquakes in Tehran. The reconstruction of two earthquakes strongly felt in Tehran in the recent years, namely that of Changureh-Avaj (22/06/2002) and Kojour (28/05/2004) provide us the occasion to study the sensitivity of our simulations and to calibrate the considered parameters. Four reasonable scenarios, were considered, including the occurrence of a strong earthquake on the Mosha, North-Alborz and Garmsar faults. For these three faults, an earthquake of magnitude MW = 7.1 was simulated. For the last one, an event with magnitude MW = 7.6, corresponding to the historical earthquake reported for this fault was also considered.*

Keywords: Empirical green function; Strong motion simulation; Tehran

1. Introduction

Investigation of seismic waveforms in broad-frequency band is one of the most important tasks in modern seismology and the outcome of such researches is indispensable for engineering seismology.

For an area of strong seismic activity like Tehran, it is possible to estimate the seismic scenarios applying various information like the historical seismicity, or of the deterministic methods using geological data on the active faults. It remains, however, much of uncertainties such as the absence of unquestionable documents on the historical seismicity and the lack of knowledge about the exact behavior of the known active faults, their kinematics, exact length and deformation velocity.

In addition, for the adapted structure design, the civil engineers need to know the complete seismogram, or at least its response spectrum. This is not directly accessible except for the well instrumented areas where a strong earthquake was already recorded. For the case of Tehran, although the important risk of major earthquakes is known by historical and geological evidences, no strong movement is still recorded.

The idea of strong motion prediction using recorded small events as Empirical Green Functions (*EGF*) was proposed first by Hartzell [14]. The method can be applied in reverse or direct problems. The reverse applications are very numerous and various, finding the focal mechanism, the source function, the complete moment tensor, or the distribution of slip on the fault [7, 8, 28, 29, 35]. Its use in direct problem is mainly intended to the simulation of the seismic movements due to a strong earthquake in future, or to strong motion estimation associated to a great earthquake occurred in the past [3, 18, 22, 24, 25, 26, 34]. The principal idea behind *EGF* method is that the weak events contain complete information on the transfer properties of the medium existing between a given source and the station (crustal propagation and the site effects).

2. Data

The data used in this study is taken from a seismological survey, conducted in the city of Tehran, from February to June 2002, in the framework of a French-Iranian collaborative project. The experiment

involved the installation of 13 portable seismological stations to record at 14 different sites, shown in Figure (1), the seismic ground motion due to earthquakes and ambient noise. Two of these stations, *JAM* and *CHA* were installed on the rock and the others over areas of different geotechnical characteristics, see Figure (1).

The main objective was the experimental estimation of the amplification effect of the local geological condition [11-12].

Five small events were selected as empirical Green functions. This choice was carried out according to the quality of the recordings, the localization of the events on or near the major faults, and finally the possibility of carrying out "calibrations" on major recorded events. Figure (2) shows the location of selected events and the major faults of the region and Table (1) shows their characteristics.

We also chose to reconstruct the seismic signal of two large events strongly felt and well recorded in Tehran to calibrate the input parameters. The first one is Changureh-Avaj earthquake (22/06/2002, *Mw* = 6.5) recorded on our temporary seismological network and the second one is Kojour (Baladeh) earthquake (21/05/2004, *Mw* = 6.3), recorded by the national accelerometric network of Iran, manipulating by Building and Housing Research Centre (*BHRC*). These two events are presented by stars with the letters *A* and *K* respectively, as shown in Figure (2).

3. Outline of the Applied Model

The method described in Pavic [30] and Pavic et al [31] was followed in this study, using the corresponding computer code. The main characteristics of the applied model are:

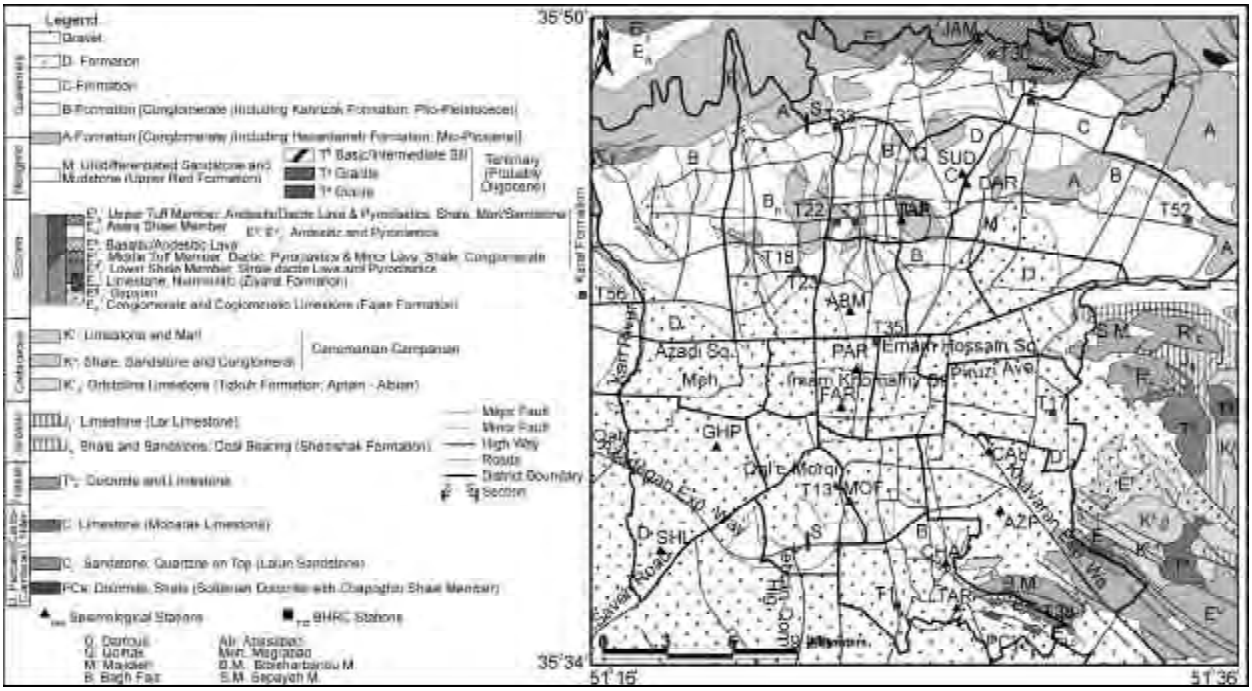

Figure 1. Location of seismological stations (triangles) used in this study. The geological base map was compiled by Jafari et al [21] based on Abbasi et al [1] and Tehran geological quaderangle (Geological Survey of Iran).

Table 1. Characteristics of the selected EGFs.

Ev.	Location	Date (y-m-d) Time (TU)	Lat. (°N)	Lon. (°E)	Depth (Km)	Mag. (M_l)	Fault of Simulation
1	SW Semnan	2002-05-13 20:49:19.0	35.385	53.117	12.2	4.4	Garmsar
2	N. Tehran	2002-03-22 04:45:27.0	35.734	51.899	16.3	2.7	Mosha
3	Alborz Central	2002-05-21 10:48:36.0	36.316	51.672	18.2	4.1	N. Alborz
4	Avaj Aftershock	2002-06-22 21:33:27.0	35.996	49.237	18	3.9	F. of Avaj Earthquake
5	Avaj Aftershock	2002-06-22 14:27:17.0	35.578	49.072	10.9	4.2	F. of Avaj Earthquake

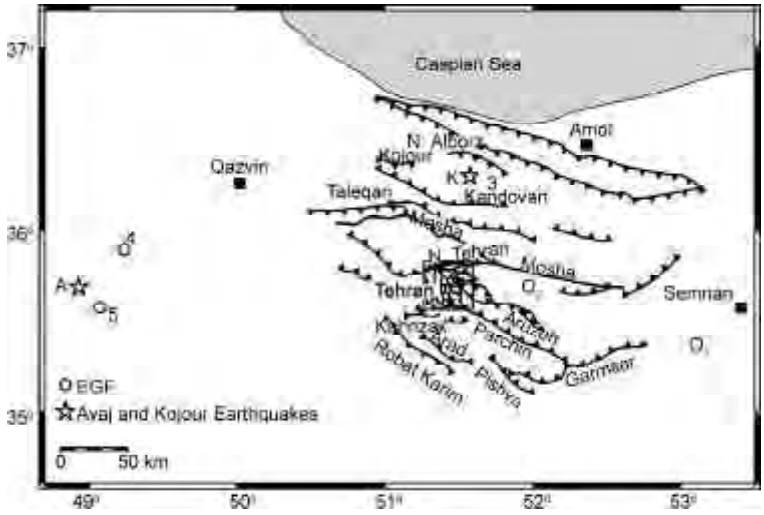

Figure 2. Location of the small events, selected as EGF with respect to the active faults of the region.

- Source model: The applied model for the present study uses a rectangular source model derived from the Kostrov crack model. The final slip at the end of the rupture is maximum in the centre of the crack, and vanishes with an ellipsoidal dependence on crack edges, while the slip function exhibits a sharp square-root discontinuity at the slip onset and a shorter total rise-time close to crack edges [31].
- Green functions summation method: There are two various families of *EGF* techniques regarding the Green function summing way. The first group is based on a statistical summation of the small events with applying a time lag between them, without trying any direct relationship to the fault plane geometry or the rupture kinematics. The only imposed condition is to respect the ω^{-2} law [34, 38]. Irikura [18-19], Bour [4] Hutchings [15], and Irikura and Kamae [20] are the representatives of the other family of *EGF* technique with a kinematic modeling of the target earthquake. The code used in this study belongs to this second family and is based particularly on work of Hutchings [15].
- Suppression of high-frequency artifacts: There is an inherent over-estimation of target/*EGF* spectral ratio with the *EGF* method for the high frequencies [5, 9, 30]. In particular, the high frequency level of the source function spectra tends to scale as $(M_0/m_0)^{1/2}$ instead of $(M_0/m_0)^{1/3}$ for the frequencies higher than corner frequency of *EGF* (*fc*). Pavic [30] proposed a specific and rather artificial processing on the high-frequency part of the source function in order to recover the theoretical ratio, $(M_0/m_0)^{1/3}$, between the complex Fourier spectra of the target simulation and the *EGF* [30-31].
- Input parameters value selection: Existing uncertainties on input parameters will be necessarily reflected on the results (accelerograms and response spectra of target earthquake among others). This difficulty had already led Hutchings et al [16] to make a parametric study which in that, instead of fixing the rupture parameters, they vary them independently by chance within the "reasonable" physically limits. A purely random selection of the various values of a parameter can not give the representative results; therefore the method known as Latin Hypercube Sampling [27] was adopted to select the various values of the parameters by Pavic [30].

4. Input Parameters Determination

The input parameters can be divided into two categories: fixed parameters and uncertain parameters. The first group is consisted of the parameters which can be given in a relatively precise way, by a single value: depth of the *EGF*, epicentral distances, source-receiver azimuth and the rigidity modulus of the crust and seismic moment of the target earthquake. The second category corresponds to the parameters (10 in total) containing an important uncertainty: strike and dip of the fault, seismic moment of the *EGF*, length of the *EGF*, fault shape factor (*L/W*) for target earthquake, stress drop of target earthquake, S-wave velocity (V_s), normalized rupture velocity V_r/V_s, and the relative rupture nucleation coordinate *X/L* and *Y/W*. For each of these parameters, it is necessary to define the probability law, which one can

choose normal, lognormal or uniform. The definition mode of most important input parameters, namely the seismic moments, fault lengths, stress drop and position of the nucleation point has been shown below in detail.

4.1 Seismic Moment

The seismic moments of the target event and that used as Green function are very important parameters because they control the number of summations to be carried out. In this study, two different relations were used to determine the seismic moment. The first is the theoretical relation connecting the seismic moment to the low frequency flat level of the displacement spectrum:

$$M_0 = 4\pi.\mu.V_s.R.W_s \tag{1}$$

In which, M_0: seismic moment in *Nm*; μ: the crust rigidity; *Vs*: mean S-waves velocity of the crust; W_s : flat level of the displacement spectrum, determined below the corner frequency and *R* is the hypocentral distance. In certain cases, the determination of the corner frequency is not easy, particularly for the small events or when the rupture mechanism is complicated. Thus, the Kanamori [23] relation was also used, which corresponds to the moment magnitude definition:

$$log M_0 = 1.5M_w + 9.1 \tag{2}$$

The magnitude scale used to characterize the selected *EGF* for most of the cases is the *Ml*. But one can consider that for magnitudes *Ml* lower than 5.5, magnitudes *Ml* and *Mw* are close together [17], a necessary but perhaps biased choice. For simulation of the main-shocks of Chnagureh-Avaj and Kojour (Baladeh) earthquakes (both of magnitude slightly higher than 6), the teleseismic seismic moments were available. The computed values reported by *USGS* were used. The seismic moment of the target event (M_0) is one of the fixed parameters and the seismic moment of the *EGF* (m_0) is defined by a lognormal distribution with a variance equal to 2 which means that 68.26% of the values of m_0 are located in the interval [*m*0/2.0, 2.0*m*0].

4.2. EGF Length

This length is supposed to follow lognormal distribution, with a variance of 1.6. The average length is determined using empirical formula of Brune [6], valid for a circular fault of ray *r* that relates the length to the corner frequency f_c of the earthquake:

$$r = 0.33\frac{V_s}{f_c} \rightarrow f_c = 0.33\frac{\sqrt{\pi}V_s}{l} \tag{3}$$

The fault is being considered as square form and its length *l* is determined by supposing that is of the same surface as the circular fault ($l = r\pi^{1/2}$). The value of the corner frequency is usually determined visually using the displacement Fourier spectra of the recorded Green functions. This visual estimation is rather delicate and subjective. The calculated length was compared with an empirical relation [39]:

$$M_w = 0.9ln(Lr) + 3.66 \tag{4}$$

In which "*Lr*" is the length of the rupture. Although there are other empirical relations such as for example that of Wells and Coopersmith [37], and that these empirical relations are valid a priori only for the earthquakes of moderate size, we considered it sufficient to use these two formulas in the estimation, taking into account the strong variance value for this parameter. In addition, our calibration study did not highlight a significant sensitivity of the results to the *EGF* length, at least in the range obtained by the various formulas.

4.3. Stress Drop

The stress drop is defined in a given point of a fault as the difference in stress state before and after the rupture. For a fault with the length *L*, of width *W* and an average slip *D*, the average stress drop is defined by:

$$D\sigma = C\mu\frac{D}{\bar{L}} \tag{5}$$

In which *C* is a "constant" (near to 1) depending on the geometry of the fault and $\bar{L}$, a characteristic dimension of the rupture (generally smallest, *W*, or the ray). One can thus relate the stress drop to seismic moment:

$$D\sigma = C'\frac{M_0}{\bar{L}^3} \tag{6}$$

In which *C'* is another constant also taking into account the relationship between width and length of the fault. Stress drop for empirical Green functions in this study is calculated theoretically according to the relation (5) by taking $C = 16/7\pi$ (circular fault) and $\bar{L} = l$. For the target earthquakes, it is defined like a fixed parameter.

4.4. Position of the Nucleation Point

The position of the nucleation point is determined

by dimensions of the fault. It is supposed that the X-coordinate of the nucleation point follows a uniform distribution on the interval [0, *L*], and its Y-coordinate, follows a uniform distribution on the interval [0, 2/3*W*]. *L* and *W* are the length and the width of the fault and the origin of axis is located in-depth on the lower edge of the fault. For Changureh-Avaj earthquake, *L* is estimated using the distribution of the aftershocks and observation of the earthquake rupture on the ground surface. For other target events, the empirical relation of Zaré [39] presented in Eq. (4) was used, while comparing with the formula rising from the scaling law that relates the seismic moment to dimensions of the fault.

$$M_0 = \mu . C_2 C_1^2 L^3 \tag{7}$$

In which, μ is the rigidity modulus of the crust (approximately $3\ 10^{10} Pa$), $C1$ and $C2$ are the constants of the scaling laws; approximately 0.5 for $C1$, and of $5\ 10^{-5}$ to 10^{-4} for $C2$. The $C1$ corresponds to the average ratio between width (W) and length (L) for the dip-slip earthquakes. This W/L ratio is defined according to a lognormal distribution with the median value 0.5 and variance of 1.3. The $C2$ corresponds to the mean ratio of average slip and the characteristic dimension of the fault, or in other words, to average stress drop.

4.5. Mechanical Parameters of the Fault and Rupture Velocity

The mean S-wave velocity at the depth of the hypocentre was fixed at 3000*m/s*, supposing that it follows a lognormal distribution, with a variance of 1.1. The rigidity modulus μ is related to S-waves velocity by the relation $\mu = \rho V_S^2$ and was considered $3\ 10^{10} N/m^2$. The rupture velocity, *Vr*, is variable and is defined through *Vr/Vs* ratio, supposing that it follows a uniform distribution on the interval [0.65, 0.95].

5. Results

In this section, first the results of calibration test, namely the simulation of Changureh-Avaj and Kojour earthquakes, are shown. Then the simulation results of an earthquake with magnitude 7.1 for 3 different faults: Garmsar, Mosha and North Alborz using the *EGF* 1 to 3, shown in Figure (2), are presented.

The calibration step reveals that the most crucial parameter is stress drop for the target earthquake. The values of $D\sigma$ lower than 10 bars, corresponding to the computed value for the Avaj earthquake by Sadeghi et al [32] up to values higher than 100 bars, were tested and the simulated response spectra were then compared with the recorded response spectra.

These comparisons showed that in order to obtain a good agreement between observations and simulations, it is necessary to choose a median stress drop value, much higher than that given by equation (5.12; at least 30 bars for Avaj earthquake and 100 bars for Kojour earthquake). It should be noted that these high values of stress drop are in agreement with the values estimated by Zaré [39] for the strong motions in Iran.

Two general remarks are essential before the detailed presentation of the results:

- Due to the high level of noise in high frequencies, it was necessary to filter the *EGF* signals. The lower filter limit was always fixed to 0.1*Hz*, but for its upper limit, it was necessary to be adapted for each case and station (almost 6-8*Hz*). The obtained results are thus valid only in these frequency bands.
- Due to the uncertainties, a great number of simulations (48 for each event at each station) were carried out. However, here only the average values and the standard deviations for the considered stations, as well as the representative simulations in time domain are presented.

5.1. Simulation of Changureh-Avaj Earthquake

The Changureh-Avaj earthquake of 22 June 2002 (02:58*GMT*) with magnitude *MW* = 6.5 (according to the *USGS*), stroke a region 200*km* west of Tehran. It claimed 261 dead, 1300 injured and a lot of damage. This earthquake, strongly felt in Tehran, occurred on a reverse fault, unknown before the quake, called Abdarreh fault, (name of a village completely destroyed) by Walker et al [36]. The main shock as well as a significant number of aftershocks were recorded by the stations installed in Tehran within the framework of this study, and can thus be used to validate the *EGF* approach and to calibrate certain input parameters.

The two aftershocks of 22 June 14:27:17 and 21:33:27, with magnitudes 4.2 and 3.9 (*ml*) respectively, were used to simulate the main-shock. The fault parameters were adapted from Walker et al [36], and also those stated by Sadeghi et al [32], Soleymani and Feghhi [33] which is summarized in Table (2).

Figure (3), for stations *MOF* and *JAM*, shows the global results of the simulation using the aftershock of 14:27.

The whole results obtained using these two after-

shocks for all stations are summarized in Table (3) in terms of maximum acceleration and Figure (4) in terms of response spectra. Figure (5) compares the simulated representative time histories with recorded ones. The values of maximum accelerations resulting from simulations are rather close to the observations,

Table 2. Input parameters for simulation of Changureh-Avaj earthquake (Mw= 6.5) using two aftershocks.

Parameter	Distribution Type	Aftershocks 14:27:17		Aftershocks 21:33:27	
		Avg.	St. Deviation	Avg.	St. Deviation
Strike (deg.)	Normal	110	20	110	20
Dip (deg.)	Normal	40	20	40	20
Long. Target (Km)	Fix	26		26	
M_0 Target (N.m)	Fix	$6.9\ 10^{18}$		$6.9\ 10^{18}$	
m_0 of EGF (N.m)	Lognormal	$2.5\ 10^{15}$	2.0	$8.9\ 10^{14}$	2.0
Long. EGF (Km)	Lognormal	1.6	1.3	1.2	1.3
Depth EGF (Km)	Fix	11		18	
$\Delta\sigma$ Target (bar)	lognormal	60	2.0	30	2.0

Table 3. Comparison of recorded peak acceleration (in m/s^2) of Changureh-Avaj earthquake simulated ones (average of 48 simulations (NS components)).

Station		ABM	CAL	CHA	JAM	MOF	SHL	TAP	SUD
Recorded Acc.		0.08	0.12	0.04	0.07	0.13	0.23	0.13	
Simulation Using Aftershock of 14:27:17	Avg.	0.13	0.08	0.07	0.08	0.19	0.27	0.17	0.17
	Representative Sim.	0.09	0.07	0.04	0.05	0.14	0.22	0.10	0.13
Simulation Using Aftershock of 21:33:27	Avg.	0.16	0.12	0.07	0.09	0.23	0.3	0.17	0.21
	Representative Sim.	0.15	0.12	0.07	0.16	0.19	0.31	0.24	0.22

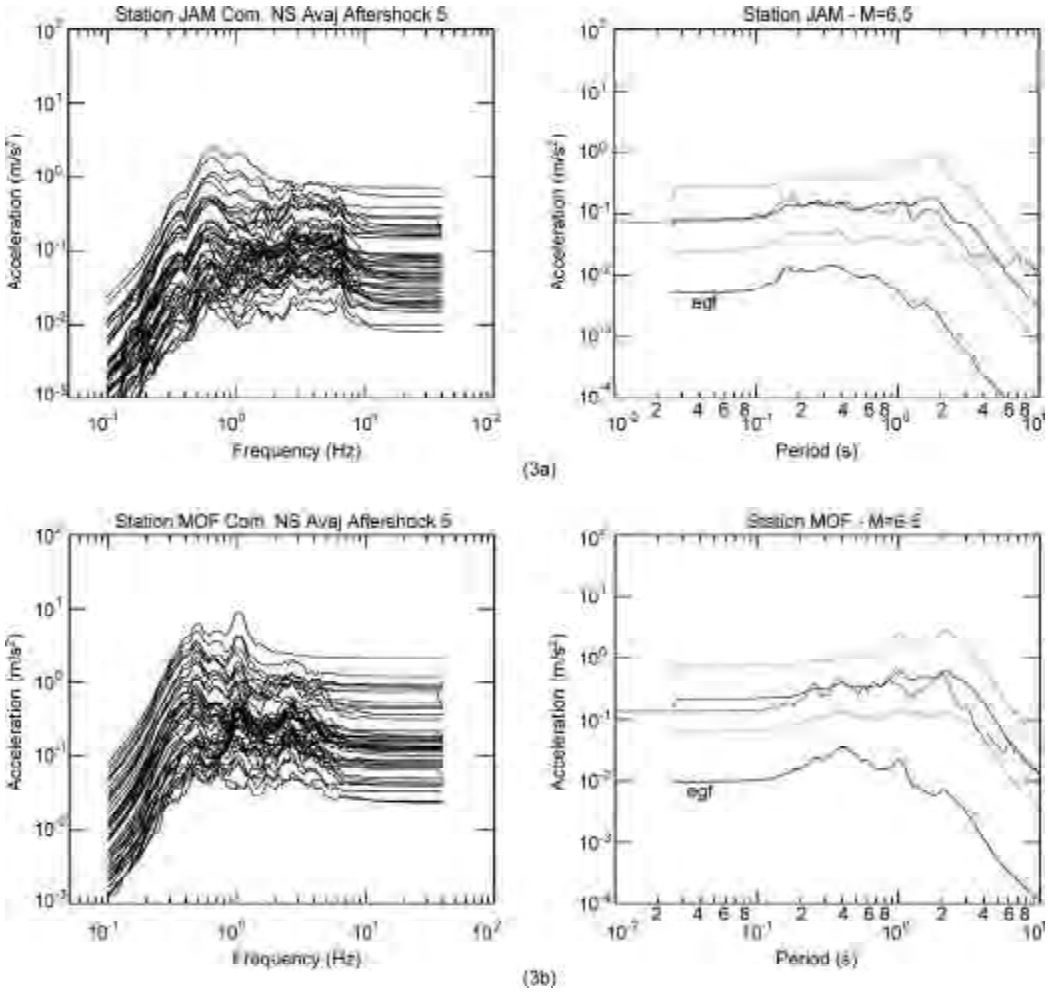

Figure 3. Simulation of Changureh-Avaj earthquake using aftershock of 22 June 2002 at 14:27:17 for NS component at JAM and MOF stations. Left plots show the response spectra of 48 simulation. The right plots compare the simulated average spectrum (continuous egf curve), its standard deviation (dotted curves), with recorded spectrum (dashed curve) and EGF spectrum (egf curve).

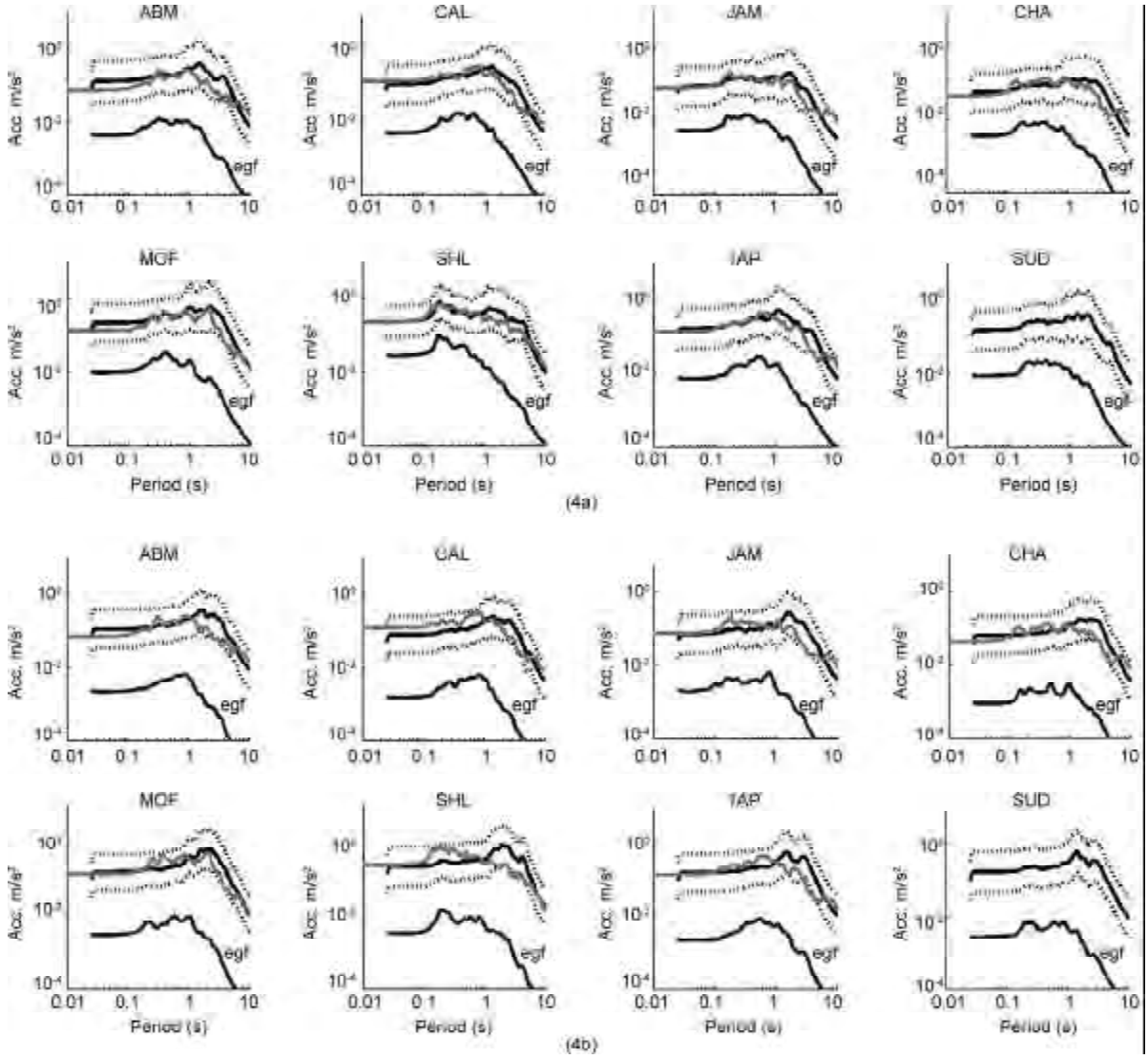

Figure 4. Simulation of Changureh-Avaj earthquake using aftershock of 22 June 2002 at (14:27:17 up), and aftershock of 22 June 2002 at 21:33:27 (down). For each station, the simulated average spectrum (continuous black curve), their standard deviations (dotted), recorded spectrum (light gray) and EGF spectrum (egf) were presented.

and reproduce well amplification effect for stations installed on the alluvial deposits comparing with the two stations installed on the rock.

5.2. Simulation of Kojour (Baladeh) and an Earthquake of Magnitude 7.1 for the North-Alborz Fault

The destroying earthquake of 28 May, 2004, known as "Kojour (Baladeh)" earthquake with magnitude *MW* = 6.3 (*USGS*), occurred in approximately 70*km* north of Tehran. This earthquake was strongly felt in Tehran with some small cracks in the buildings in the north-western part of the city. This earthquake was recorded by many accelerometers installed in Tehran by *BHRC* within the framework of the national accelerometer network of Iran.

Supposing the North-Alborz fault as a causative fault for this earthquake, we could make a scenario for the occurrence of a larger earthquake on this fault.

The event of 21 May 2002 (10:48:36.0) was chosen as *EGF* to reconstruct the Kojour earthquake for the sites studied during this project. This earthquake had a magnitude *ml* = 4.1, and the epicenter close to that of Kojour earthquake. The input parameters of simulation are presented in Table (4). The fault parameters were selected based on Ghaitanchi [10].

The simulated response spectra for each station of our temporary network are compared to observe response spectra at the nearest *BHRC* stations, see Figure (6) and Table (5). For *CHA* station, we compared the result to Teh17 and Teh38 stations installed on the rock in the east and the south of the city. This comparison reveals a good agreement between simulations and the observation particularly

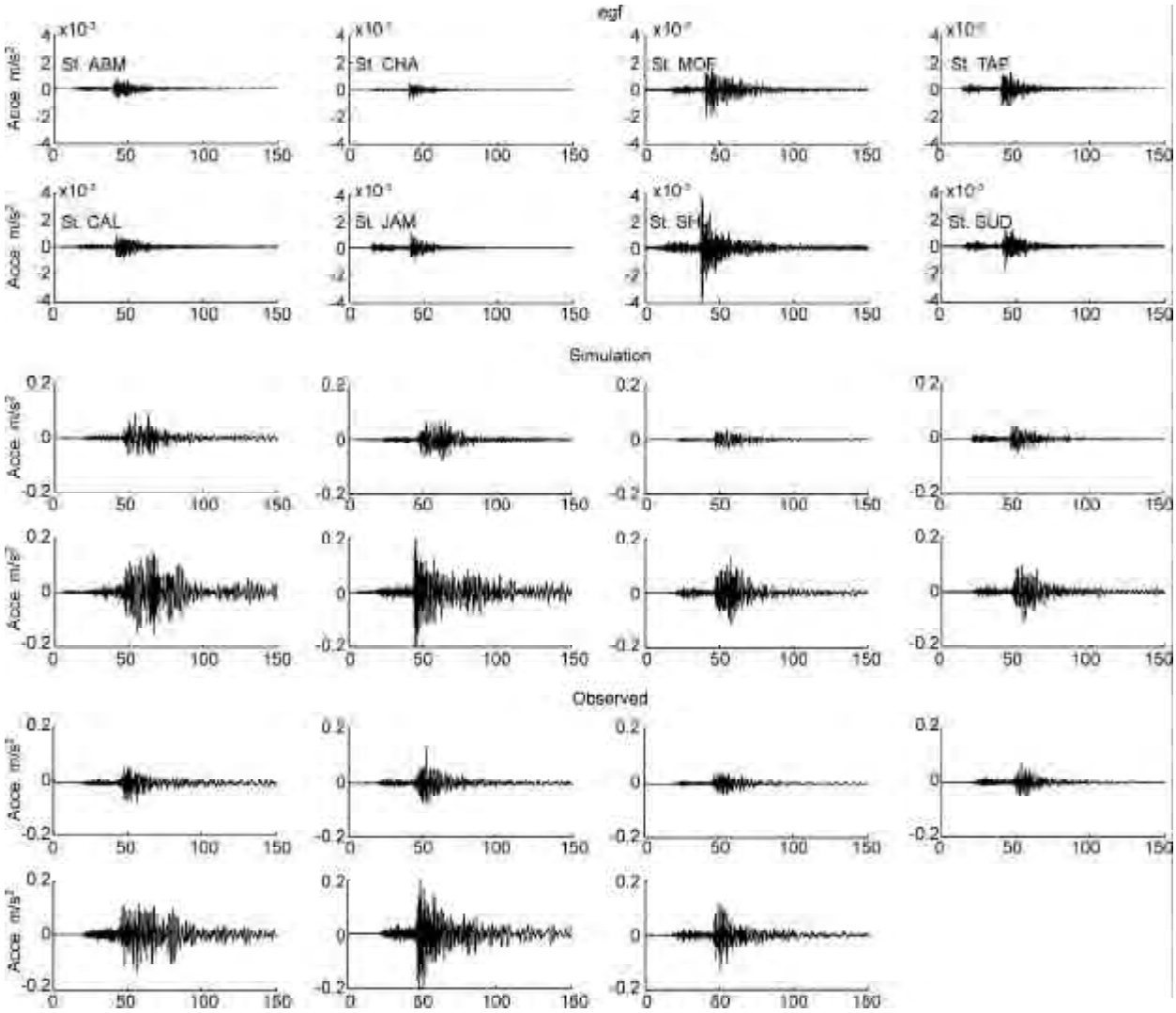

Figure 5. Comparison of accelerograms obtained from simulation n°34 (among 48) of Changureh-Avaj earthquake (middle) using aftershock of 22 June 2002 at 14:27:17, with EGF (up) and recorded ones (down). Scale of accelerations changes between EGF and simulated and the recorded mainshock.

Table 4. Input parameters for the simulation of Kojour earthquake and an earthquake of MW = 7.1 on North-Alborz fault using an event of ml = 4.1 located near the epicenter of Kojour earthquake.

Parameter	Distribution Type	Simulation of Mw = 6.3		Simulation of Mw = 7.1	
		Avg.	Std	Avg.	Std
Strike (deg.)	Normal	120	20	120	20
Dip (deg.)	Normal	50	20	50	20
Target Long. (Km)	Fix	20		46	
M_0 Target (N.m)	Fix	$3.65\ 10^{18}$		$5.63\ 10^{19}$	
M_0 of EGF (N.m)	Lognormal	5.71e14	2.0	$5.71\ 10^{14}$	2.0
Long. EGF (Km)	Lognormal	0.723	1.3	0.723	1.3
Depth EGF (Km)	Fix	18.2		18.2	
$\Delta\sigma$ Target (bar)	Lognormal	70	2.0	70	2.0

Table 5. Average of maximum accelerations (cm/s²) of 48 simulations for two different scenarios on North-Alborz fault, and recorded values on the closest BHRC sites (component NS).

BHRC Site	Teh01	Teh38	Teh33	Teh13	Teh30	Teh13	Teh35	Teh13	Teh11	Teh01
Acc.	27.7	8.5	15.6	28.5	16.8	28.5	16.4	28.5	27.3	27.7
Station	AZP	CHA	DAR	GHP	JAM	MOF	PAR	SHL	TAP	TAR
Simulated Kojour Eq.	20.7	8.5	54.9	22.5	29.8	24.6	13.1	41.5	41.7	21.1
Simulated Mw = 7.1	51.9	19.0	109.1	56.1	63.4	66.8	29.0	81.2	83.2	54.2

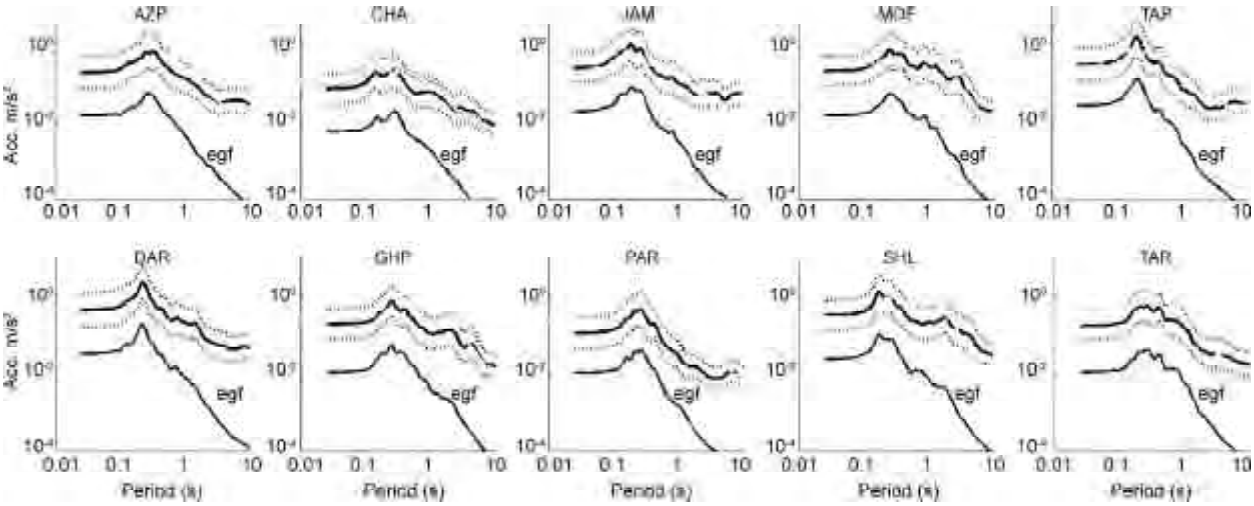

Figure 6. Simulation of Kojour earthquake. For each station, the average simulated response spectrum (continuous black curve), their standard deviations (dotted lines), the response spectrum of the EGF (egf) and the recorded spectrum (light gray) on nearest BHRC site are superimposed. BHRC sites corresponding to each station is indicated in Table (5). Stations TAP and PAR were equipped with the sensor L22 (2Hz); thus simulations are only valid beyond this frequency.

for four sites (*CHA*, *MOF*, *TAP* and *JAM*) when a stress drop of 70 bars was used. This value of stress drop is very close to the value of 64 bars calculated by Ghaitanchi [10].

Stations *AZP* and *TAR* show response spectra lower than recorded one on the Teh01 station located at the west of *TAR*. This difference is in agreement with the result of site effect study in Tehran [11-12] concerning the increase of amplification towards the west for the southern part of the city.

The increase of the response spectra at low frequency for stations *PAR* and *TAP* comes owing to the fact that these stations were equipped with *L*22 (2*Hz*) sensors. Therefore, the obtained results are valid only beyond this frequency.

After this calibration test, an earthquake with magnitude 7.1 on the North-Alborz fault was simulated. The results are summarized in Figures (7) and (8), and the average values of maximum acceleration of 48 simulations are presented in Table (5). In addition to aforementioned remarks about the simulation of the Kojour earthquake, the observation of the maximum acceleration values as well as response spectra leads to another significant result, namely strong high frequency amplification for *DAR* station (compared to *JAM*). It results in acceleration higher than 0.1*g* in the time domain and a spectral acceleration of 0.4*g* for periods between 0.2 and 0.3*sec*.

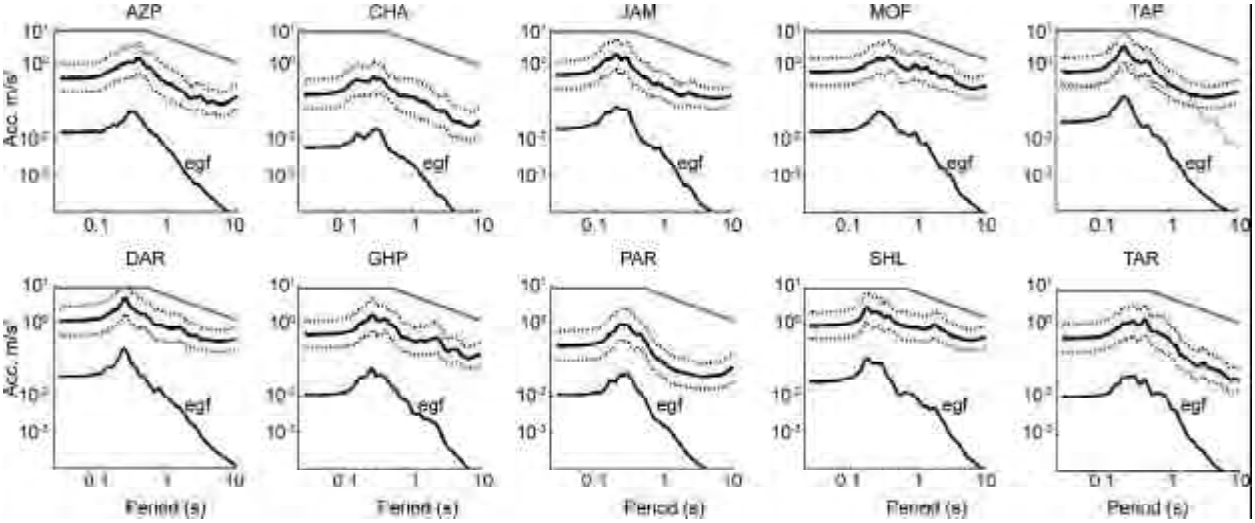

Figure 7. Average response spectra (continuous black) and their standard deviation (dotted) resulting from the simulation of an earthquake of MW = 7.1 on the North-Alborz fault in an epicenteral distance from 54 to 84km. The spectra are compared with those of the EGF used (egf) and those proposed by the Iranian building code (light gray).

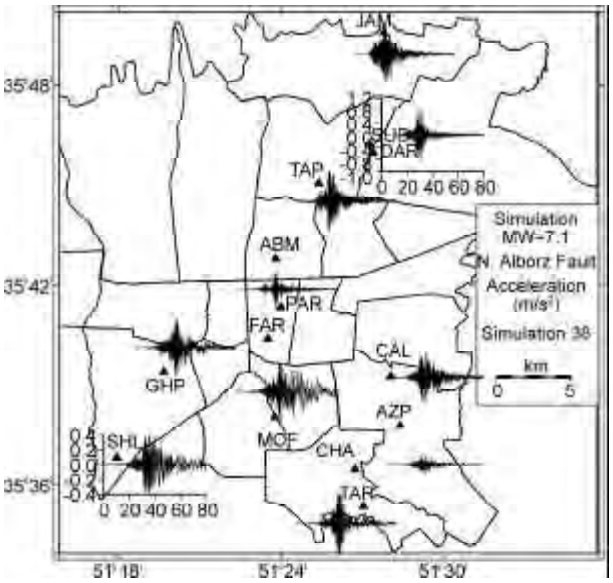

Figure 8. Example of simulation for an earthquake of magnitude 7.1 on the North- Alborz fault (simulation 38 among the 48). The scale of traces for all stations is like SHL, except for DAR station.

The obtained response spectra are compared with those of the Iranian construction code by considering appropriate type of ground for each station. It can be seen that the simulated spectra are well below the proposed standard, which is normal for such a epicentral distance. However, for some stations like *SHL*, *MOF* and particularly *DAR*, the spectral values approach the code values.

5.3. Simulation of the Earthquakes of Magnitude 7.1 and 7.6 on the Garmsar Fault

This scenario was chosen for 2 reasons: on the one hand the fault of Garmsar is an active fault considered as the origin of one of the largest historical earthquake in the area, $Ms \sim 7.6$, 3rd century *BC* [2]. In addition, one of our best recorded events, the South-west Semnan earthquake (13/05/2002, $Ml = 4.4$), with a very good signal-to-noise ratio, on almost all the stations was located on the east prolongation of this fault. This opportunity enables us to make a simulation on a rather broad frequency band. The input parameters are listed in Table (6), and the results of simulation are summarized in Figures (9), (10) and Table (7). The stress drip for the target earthquake is considered 70 bars as the North-Alborz scenario. The response spectra are compared at the same time with the proposed spectra in the Iranian building code and those of aforementioned simulation on the North-Alborz. It can be seen that in spite of the relatively large epicenteral distance (150*km*), the spectral values are rather high and comparable with

Table 6. Input parameters used for the simulation of an earthquake of MW=7.1 on Garmsar fault using an earthquake of ml=4.4, located in the south-west of Semnan.

Parameter	Distribution Type	Avg.	Std
Strike (Deg.)	Normal	250	20
Dip (Deg.)	Normal	45	20
Target Long. (Km)	Fix	46	
M_0 Target (N.m)	Fix	$5.63\ 10^{19}$	
M_0 of EGF (N.m)	Lognormal	$8.85\ 10^{14}$	2.0
Long. EGF (Km)	Lognormal	1.245	1.3
Depth EGF (Km)	Fix	12.2	
$\Delta\sigma$ Target (Bar)	Lognormal	70	2.0

those of the North-Alborz scenario for the sites in the south-east of the city.

This remark is important, because in the case of reactivation of the western segments of this fault, one can thus expect strong movements in *SE* sector of the city. It is at *AZP* station that the simulated acceleration has the highest value ($87 cm/s^2$) and that of *DAR* remaining still rather high also for this scenario. We chose $Mw = 7.1$ magnitude for the target event to remain within the limits of the validity of the similarity law; but also carried out a test for $Mw = 7.6$ corresponding to the historical earthquake attributed to this fault. The results are presented in Figure (11) in terms of average response spectra, which shows that in this case, the simulated spectra approach the building code proposed spectra for the stations installed in the south of the city, as well as for station *DAR* in the north.

5.4. Simulation of an Earthquake of Magnitude 7.1 on the Mosha Fault Using an EGF of Ml = 2.9 (22/03/2002)

For the last scenario, a small earthquake of magnitude 2.9, located near to the Mosha fault, was chosen. The goal was to simulate the effect of a strong earthquake at an epicentral distance near to the city. This fault was currently far from active, and only a small $Ml = 2.9$ event was available, for which the weakness of the signal/noise ratio led us to use only the recordings of four stations *AZP*, *CHA*, *DAR* and *TAR* (*JAM* station was broken down at the time). Moreover, for *DAR* station, a low pass filtering below 4*Hz* was carried out due to the high frequency noises. The results of simulation for this site are thus valid only for lower frequencies.

Considering the important difference in magnitude between the target earthquake and the *EGF*, the direct simulation was not possible in the current version of the program. An intermediate step, was thus chosen including the simulation of an earthquake

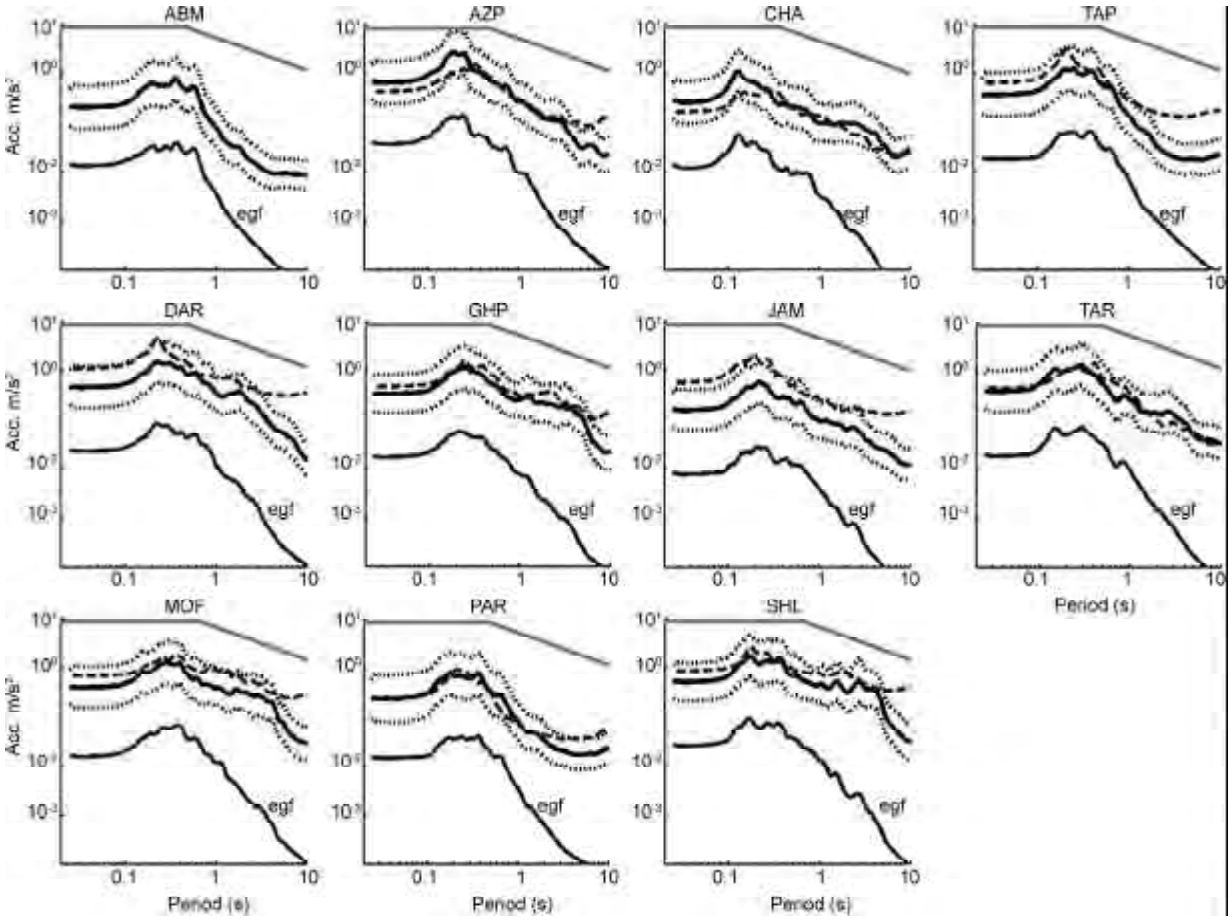

Figure 9. Average response spectra (continuous black) and their standard deviation (dotted) resulting from the simulation of an earthquake of MW=7.1 on the Garmsar fault. The response spectra are compared with those of the EGF used (egf), those proposed by the Iranian building code (light gray) and with the response spectra, simulated for an earthquake of magnitude 7.1 on North-Alborz fault (dashed lines). Stations ABM, TAP and PAR were equipped with the L22 (2Hz) sensors.

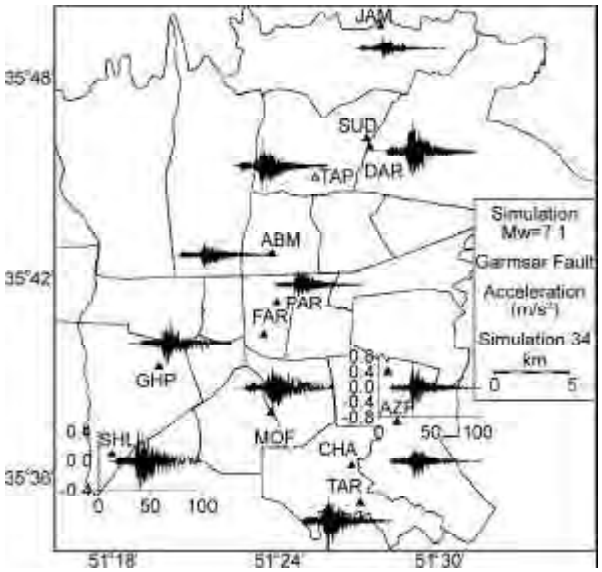

Figure 10. Example of simulation of an earthquake of magnitude 7.1 on the Garmsar fault (simulation N°34 among 48). The scale of the traces is identical to SHL station, except for AZP station.

Table 7. Comparison of maximum simulated accelerations (cm/s^2) for the component NS (means of 48 simulations) using the south-west Semnan earthquake.

Station	ABM	AZP	CHA	DAR	GHP	JAM	MOF	PAR	SHL	TAP	TAR
Mw = 7.1	26	85	30	60	40	20	50	30	60	45	50
Mw = 7.6	40	135	50	100	70	30	80	50	100	70	70

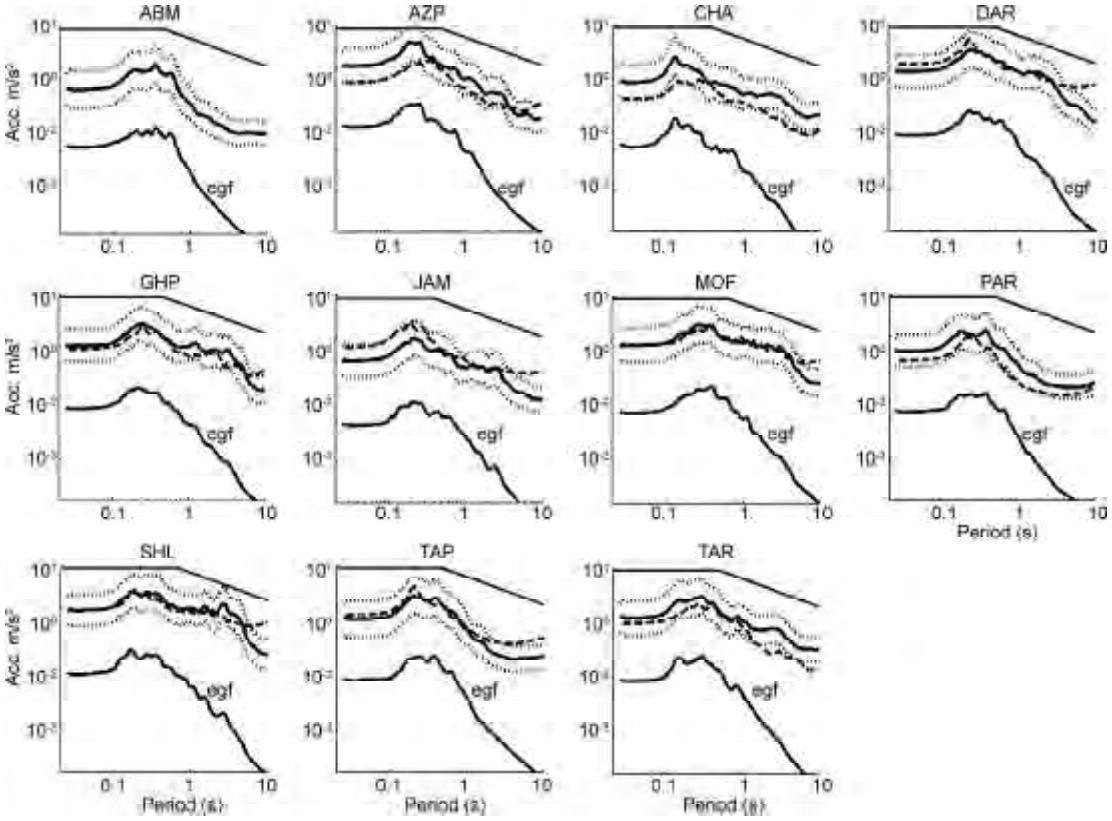

Figure 11. Average response spectra (continuous black curve) and their standard deviation (dotted lines) resulting from the simulation of an earthquake of MW = 7.6 on the Garmsar fault. The spectra are compared with those of the EGF used (egf), those proposed by the Iranian building code (light gray) and those simulated for an earthquake of magnitude 7.1 on North-Alborz fault (dashed lines). Stations ABM, TAP and PAR were equipped with the L22 (2Hz) sensors.

of magnitude $MW = 5$. The input parameters are presented in Table (8) and the results of simulation are summarized in Figures (12) and (13). The second step simulation is carried out using the simulation number 34 obtained from the first step, which shows a response spectrum very close to the average of 48 simulations.

As the results reveal, for the alluvial sites, the response spectra approach very much to the building code proposed spectrum for certain frequencies, and the values [average plus standard deviation] exceeded almost systematically the proposed values. Considering that the sites presented for this simulation are not the sites with high amplification, see [12], one can expect much more exceedence in the case of high amplifying site such as *MOF* and *SHL*. It is necessary however, to keep in mind that for an earthquake of magnitude 7.1 at a near epicentral distance (40*km*), the length of fault is important, and the forms of signals emitted by the various points of the fault can strongly vary, since, a correct simulation require the use of more number of *EGFs*.

Table 8. Input parameters used for the simulation of the earthquakes of magnitude 5.0 and 7.1 on the Mosha fault using an earthquake of ml = 2.9.

Parameter	Distribution Type	Simulation of Mw = 5.0		Simulation of Mw = 7.1	
		Avg.	Std	Avg.	Std
Strike (Deg.)	Normal	290	20	290	20
Dip (Deg.)	Normal	50	20	50	20
Target Long. (Km)	Fix	4.4		46	
M_0 Target (N.m)	Fix	$4.0\ 10^{16}$		$5.62\ 10^{19}$	
M_0 of EGF (N.m)	Lognormal	$1.41\ 10^{13}$	2.0	$4.0\ 10^{16}$	1.0
Long. EGF (Km)	Lognormal	0.2	1.3	4.4	1.3
Depth EGF (Km)	Fix	16.3		16.3	
$\Delta\sigma$ EGF (Bar)	Lognormal	70	2.0	70	2.0

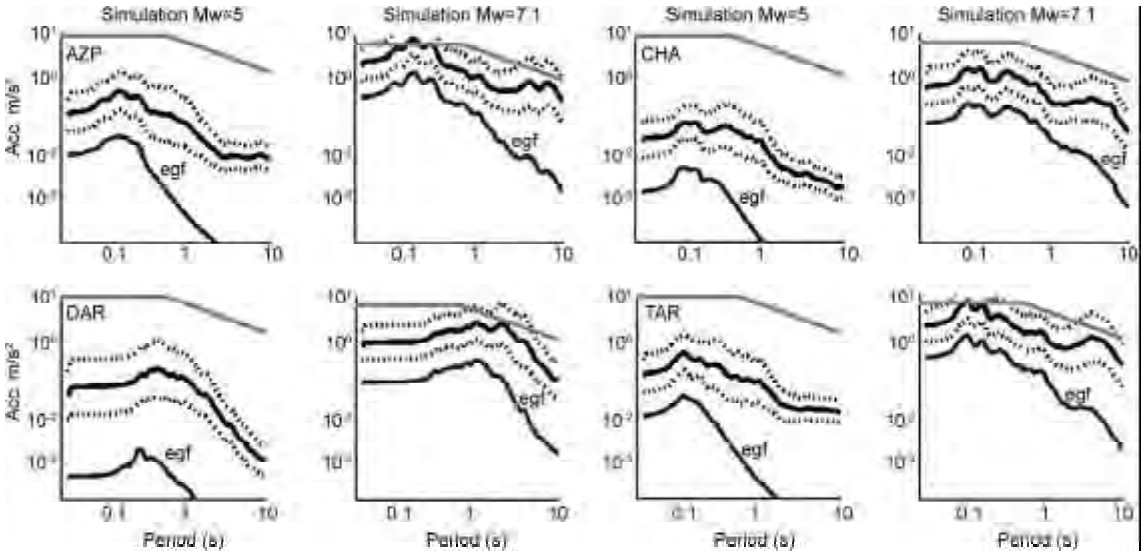

Figure 12. Simulation of an earthquake of magnitude 7.1 on the fault of Mosha using a small event of M=2.9, in two stages (2.9 → 5.0 and 5.0 → 7.1). Average response spectra (continuous black curve), their standard deviation (dotted lines), response spectra of EGF (dark gray) and those proposed by the Iranian code (light gray) are presented.

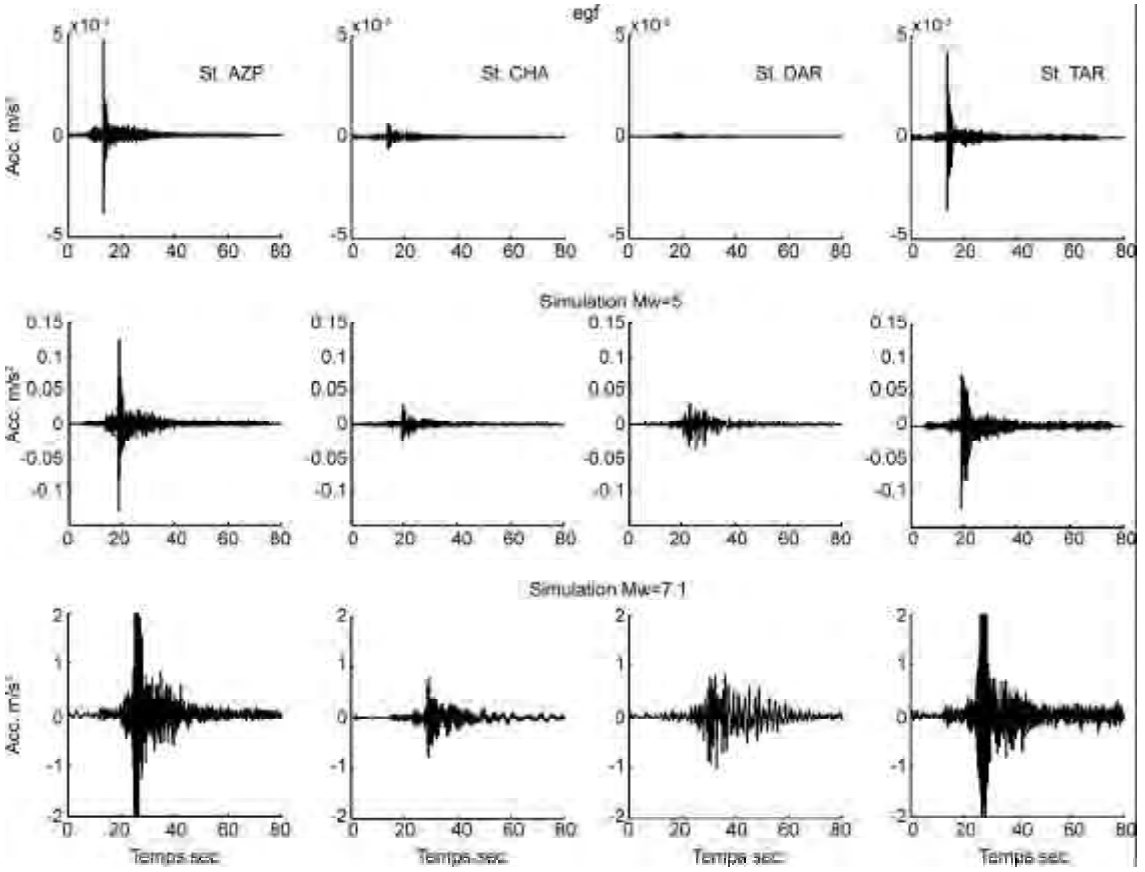

Figure 13. Example of simulation of an earthquake of magnitude 7.1 on the fault of Mosha: Traces of the EGF (left) and representative traces obtained for the two stages of simulation (Mw=5 in the middle, and Mw=7.1 on the right).

6. Conclusion

This study was carried out to predict the effect of a strong motion within the city of Tehran for various scenarios, by using small recorded earthquake as the empirical Green functions. Initially, to calibrate the calculation, two large events, those of Changureh-Avaj and Kojour, strongly felt and recorded well in Tehran, were simulated using two aftershocks for the former, and an event of magnitude 4.1 which has

occurred in 21/05/2002 for the latter. This step showed that the choice of the stress drop for the target events is of primary importance, and can significantly change the results of simulation. After various tests with variable stress drops, the values between 30 and 70 bars led to the most similar results with the real recordings. Then, three different scenarios were considered to the occurrence of an earthquake of magnitude 7.1 on the faults, North-Alborz, Garmsar and Mosha using small events, supposedly generated by these faults. For the fault of Garmsar, we also simulated a larger event (Mw = 7.6) corresponding to the largest historical earthquake, attributed to this fault. The results of these four scenarios are presented in Tables (9) and (10) in terms of maximum acceleration in the time domain, and of spectral acceleration for three different frequencies (0.5, 1 and 3Hz).

These values prove rather significant (i.e. likely to cause damage), even at relatively large epicentral distances. These results are in agreement with another study on seismic strong motion estimation for Tehran based on synthetic signals computed by an hibrid method [13]. For example, maximum esimulated acceleration for *AZP* station in the case of an event of MW = 7.1 on the Mosha fault (distance of 40km) is of 0.34g, identical to that given by the Iranian building code (0.35g).

For this last scenario, the values of spectral acceleration for high frequency (10Hz) was also presented for three stations filtered below 15Hz. These results show a very important spectral acceleration for *AZP* and *TAR* stations (approximately 1g for *AZP*). These values can be very important if we consider that these two stations are installed in districts where most of the existing buildings are of one or two storeys, and are thus characterized by a rather high natural frequency (5 to 10Hz).

In the frequency domain, the response spectra was also compared with those proposed by the Iranian building code. For the first two scenarios, the simulated spectra remained smaller than the code spectra, but could be exceeded for the scenario of Mosha. These observations, along with the fact that the maximum potential magnitudes for the faults in the region are higher than 7.1 (7.6 for Garmsar, and for example), as well as the existence of active faults at very short distance (North-Teheran, for example), all made us think that certain earthquakes can produce motions which significantly exceeds the current Iranian code, especially due to the important site effects in Tehran.

Table 9. Average peak accelerations estimated using the Empirical Green Function technique for the component NS (cm/s^2) in various sites of Tehran, for an earthquake of magnitude 7.1 located on the faults of North-Alborz, Garmsar and Mosha.

Station	ABM	AZP	CHA	DAR	GHP	JAM	MOF	PAR	SHL	TAP	TAR
North-Alborz		50	20	110	55	60	65	30	80	85	55
Garmsar Mw = 7.1	26	85	30	60	40	20	50	30	60	45	50
Garmsar Mw = 7.6	40	135	50	100	70	30	80	50	100	70	70
Mosha		340	80	110							280

Table 10. Average spectral accelerations were estimated using the Empirical Green Function technique for the component NS (cm/s^2) in various sites of Tehran in various scenarios.

Station	Fr. (Hz)	ABM	AZP	CHA	DAR	GHP	JAM	MOF	PAR	SHL	TAP	TAR
N. Alborz	0.5		12	7	45	37	16	54	4	78	16	10
	1.0		32	14	70	32	27	93	7	76	28	35
	3.0		149	43	210	116	97	162	57	144	127	99
Garmsar Mw = 7.1	0.5	2	12	10	33	21	6	32	3	31	3	14
	1.0	8	27	10	35	26	10	38	9	45	14	26
	3.0	64	117	28	136	95	30	118	66	135	96	107
Garmsar Mw = 7.6	0.5	5	23	21	62	44	14	65	8	64	9	31
	1.0	15	52	21	70	54	17	75	19	93	30	52
	3.0	105	180	45	213	153	47	191	107	216	143	167
Mosha	0.5		61	30	258							65
	1.0		101	29	254							110
	3.0		250	138	193							262
	10.0		945	169								695

Acknowledgments

This work was made possible through a PhD fellowship partially granted by the French embassy in Tehran and research funds allocated by various French agencies: *CNRS*, *ACI-RNCC*, National Research Agency and also *IIEES* logistic support in Iran.

References

1. Abbasi, M.R. and Shabanian Boroujeni, E. (2005). "Determination of Stress State and Direction by Inversion of Fault-Slip Data in the Southern Flank of Central Alborz", *Scientific Quarterly Journal of Geosciences*, Geological Survey of Iran, **12**(55), (In Persian).

2. Ambraseys, N.N. and Melville, C.P. (1982). "A History of Persian Earthquakes", Cambridge Earth Science Series, Cambridge University Press, London, 212p.

3. Boatwright, J. (1988). "The Seismic Radiation from Composite Models of Faulting", Bull. Seism. Soc. Am., **78**(2), 489-508.

4. Bour, M. (1993). "Simulation de Forts Mouvement Du Sol à Partir de Petits Séismes Utilises Comme Fonctions de Green Empiriques", Thèses de Doctorat, Uni. Louis Pasteur, Strasbourg, France.

5. Bour, M. and Cara, M. (1997). "Test of a Simple Empirical Green's Function Method on Moderatesized Earthquakes", Bull. Seism. Soc. Am., **87**(3), 668-683.

6. Brune, J. (1970). "Tectonic Stress on the Spectra of Seismic Shear Waves from Earthquakes", *J. Geophys. Res.*, **75**, 4997-5009.

7. Courboulex, F., Singh, S.K., Pacheco, J.F., and Ammon, C.J. (1997). "The 1995 Colima-Jalisco, Mexico, Earthquake (Mw8): A Study of the Rupture Process", *Geoph. Res. Lett.*, **24**, 1019-1022.

8. Frankel, A., Fletcher, J., Vernon, F., Haar, L., Berger, J., Hanks, T., and Brune, J. (1986). "Rupture Characteristic and Tomographic Source Imaging of ML~3 Earthquakes Near Anza Southern California", *J. Geophys. Res.*, **91**, 12633-12650.

9. Gariel, J.C. and Mohammadioun, B. (1991). "Simulation des Mouvements Forts Par la Technique Des Fonction de Green Empiriques", Note Technique SERGD/91/41, IPSN, SERGD, Fontenay-Aux-Roses, France.

10. Gheitanchi, M.R. (2004). "Analysis of the 28th May 2004 Baladeh-Kojur Earthquake in Mazandaran Province", http://seismo.um.ac.ir/conference/abstract_eng.pdf.

11. Haghshenas, E., Bard P.Y., Jafari, M.K., and Hatzfeld, D. (2003). "Effets de Site et Risque Sismique à Téhéran : Premiers Résultats D'une Etude Expérimentale", 6ème Colloque National AFPS, Association Française de Génie Parasismique, Paris.

12. Haghshenas, E. (2005). "Aléa Sismique et Condition Géotechnique à Téhéran", Ph.D. Thesis, University of Joseph Fourier, Grenoble-France, (In French).

13. Hamzehloo, H., Vaccari, F., and Panza, G.F. (2007). "Towards a Reliable Seismic Microzonation in Tehran, Iran", *Engineering Geology*, **93**, 1-16.

14. Hartzell, S.H. (1978). "Earthquake Aftershocks as Green's Functions", Geophys. Res. Lett., **5**(1), 1-4.

15. Hutchings, L.J. (1994). "Kinematic Earthquake Models and Synthesized Ground Motion Using Empirical Green's Functions", Bull. Seism. Soc. Am., **84**(4), 1028-1050.

16. Hutchings, L.J., Japre, S.P., Kasmeyer, P.W., and Foxall, W. (1996). "Synthetic Strong Ground Motion for Engineering Design Utilising Empirical Green's Functions", *Proceeding 11th World Conf. on Earthquake Engineering*, Acapulo.

17. Idriss, I.M. (1985). "Evaluating Seismic Risk in Engineering Practice", *Proc., 11th International Conference on Soil Mechanics and Foundation Engineering*, San Francisco, Balkema, Rotterdam, 265-320.

18. Irikura, K. (1983). "Semi-Empirical Estimation of Strong Ground Motions During Large Earthquakes", Bull. Disas. Prev. Res. Inst., Kyoto Univ., 33, Part 2, No. 298, 63-104.

19. Irikura, K. (1986). "Prediction of Strong Acceleration Motions Using Empirical Green's Functions", *Proc. 7th Japan Earthquake Eng.*

Symp., 151-156.

20. Irikura, K. and Kamae, K. (1994). "Estimation of Strong Ground Motions in Broad-Frequency Band Based on Seismic Source Scaling Model and Empirical Green's Functions Technique", Annali di Geofisica, **37**(6), 1721-1743.

21. Jafari, M.K., Razmkhah, A., Keshavarz-Bakhshayesh, M., Sohrabi, A., and Pourazin, Kh. (2001). "Complementary Studies of the Earthquake Geotechnical Microzonation in South of Tehran", IIEES, Spec. Pub. (In Persian).

22. Joyner, W. and Boore, D.M. (1986). "On Simulating Large Earthquakes by Green's Function Addition of Smaller Earthquakes", Earthquake Source Mechanics", Geophysical Monograph, **37**, Am. Geophys. Union, **6**, 269-274.

23. Kanamori, H. (1977). "The Energy Release in Great Earthquakes", *J. Geophys. Res.*, **82**, 2981-2987.

24. Kanamori, H., Jennings, P.C., Singh, S.K., and Astiz, L. (1993). "Estimation of Strong Ground Motions in Mexico City Expected for Large Earthquakes in the Guerrero Deismic Gap", Bull. Seism. Soc. Am., **83**, 811-829.

25. Lachet, C. (1996). "Observation des Séismes en Milieux Urbains: Méthodes Simple D'étude Des Effets de Site et de Simulation Des Mouvement Forts", Thèse de Doctorat, Université Joseph Fourier, Grenoble, France.

26. Lebrun, B. (1997). "Les Effet de Site: Etude Expérimentale et Simulation de Trois Configurations", Thèse de Doctorat, Université Joseph Fourier, Grenoble, France.

27. McKay, M.-D. (1988). "Sensitivity and Uncertainty Analysis Using a Statistical Sample of Input Values", Uncertainty Analysis, ed. Yigal Ronen, CRC Press, Florida, U.S.A.

28. Mori, J. and Frankel, A. (1990). "Source Parameters for Earthquakes Associated with the 1986 North Palm Springs, California, Earthquake Determined Using Empirical Green Functions", Bull. Seism. Soc. Am., **80**, 278-295.

29. Mueller, C.S. (1985). "Source Pulse Enhancement by Deconvolution of an Empirical Green's Function", Geoph. Res. Lett., **12**, 33-36.

30. Pavic, R. (1997). "Méthode des Fonctions de Green Empiriques, Etude de Sensibilité en vue Dune Application en Ingénierie", Diplôme D'ingénieur de L'Ecole de Physique du Globe de l'Université de Strasbourg I.

31. Pavic, R., Koller, M.G., Bard, P.Y., and Lacave-Lachet, C. (2000). "Ground Motion Prediction with Green's Function Technique: An Assessment of Uncertainties and Confidence Level", *Journal of Seismology*, **4**, 59-77.

32. Sadeghi, H., Suzuki, S., Hosseini, S.K., Fujii, Y., and Fatemi Aghda, S.M. (2003). "Estimation of Earthquake Source Parameters of the June 22, 2002 Changureh-Avaj Event, NW Iran, Using Aftershocks Distribution and Far-Field Data", Geophys. Res. Abs., **5**, 07098.

33. Soleymani, Sh. and Feghhi, Kh. (2003). "Report of Surface Faulting and Morphotectonics of 'Avaj Region' Earthquake on 22 June 2002", Website: www.iiees.ac.ir.

34. Tumakrin, A.G. and Archuleta, R.J. (1994). "Empirical Ground Motion Prediction", Annali di Geofisica, **37**(6), 1691-1720.

35. Velasco, A.A., Ammon, C.J., and Lay, T. (1994). "Empirical Green Function Deconvolution of Broad-Band Surface Waves: Rupture Directivity of the 1992 Landers, California (Mw = 7.3)", Bull. Seism., Soc. Am., **84**, 735-750.

36. Walker, R., Bergman, E., Jackson, J., Ghorashi, M., and Talebian, M. (2005). "The 2002 June 22 Changureh (Avaj) Earthquake in Qazvin Province, Northwest Iran: Epicentral Relocation, Source Parameters, Surface Deformation and Geomorphology", *Gheophys. J. Int.*, **160**, 707-720.

37. Wells, D.L. and Coppersmith, K.J. (1994). "New Empirical Relationships Among Magnitude, Rupture Length, Rupture Width, Rupture Area, and Surface Displacement", Bull. Seismol. Soc. Am., **84**, 974-1002.

38. Wennerberg, L. (1990). "Stochastic Summation of Empirical Green's Function", Bull. Seism. Soc. Am., **80**(6), 1418-1432.

39. Zaré, M. (1999). "Contribution à L'étude Des Mouvement Forts en Iran; Du Catalogue Aux Lois D'atténuation", Thèse de Doctorat, Université Joseph Fourier, Grenoble, France.